

# Long-term inhibition of UCHLI decreases hypertension and retinopathy in spontaneously hypertensive rats

Journal of International Medical Research

49(6) 1–14

© The Author(s) 2021

Article reuse guidelines:

sagepub.com/journals-permissions

DOI: 10.1177/03000605211020641

journals.sagepub.com/home/imr



Shasha Liu<sup>1,2</sup> , Chengfang Wang<sup>2</sup>,  
Jianmin Lu<sup>3</sup>, Guangzheng Dai<sup>4</sup>, Huixin Che<sup>4</sup>  
and Wei He<sup>1,4</sup>

## Abstract

**Objective:** To investigate the role of the deubiquitinase ubiquitin C-terminal hydrolase LI (UCHLI) in hypertension and retinopathy in the spontaneously hypertensive rat (SHR).

**Methods:** Wistar–Kyoto (WKY) rats and SHRs were administered the UCHLI inhibitor LDN57444 (20 µg/kg/day) for 4 months. Pathological changes were detected with hematoxylin and eosin, immunofluorescence, and dihydroethidium staining. The mRNA and protein expression of UCHLI were examined by real-time PCR and immunoblotting analysis.

**Results:** At 6 months of age, SHRs showed significantly increased mRNA and protein levels of UCHLI in the retina compared with WKY rats. Moreover, SHRs exhibited significantly increased central retinal thickness, inflammation, and reactive oxygen species production compared with WKY rats, and these effects were markedly attenuated by systemic administration of the UCHLI inhibitor LDN57444. The beneficial effects of LDN57444 were possibly associated with reduced blood pressure and the inactivation of several signaling pathways.

**Conclusion:** UCHLI is involved in hypertension and retinopathy in SHRs, suggesting that UCHLI may be used as a potential therapeutic target for treating hypertensive retinopathy.

<sup>1</sup>The Second Clinical College, Dalian Medical University, Dalian, P.R. China

<sup>2</sup>Health Management Center, First Affiliated Hospital of Dalian Medical University, Dalian, P.R. China

<sup>3</sup>Department of Ophthalmology, First Affiliated Hospital of Dalian Medical University, Dalian, P.R. China

<sup>4</sup>Clinical Research Center, He Eye Specialists Hospitals, Shenyang, P.R. China

## Corresponding author:

Wei He, The Second Clinical College, Dalian Medical University, 467 Zhongshan Road, Dalian 116023, P.R. China.

Email: hewei05@hsyk.com.cn



## Keywords

Hypertension, retinopathy, ubiquitin C-terminal hydrolase L1, inflammation, oxidative stress, therapeutic target

Date received: 5 October 2020; accepted: 7 May 2021

## Introduction

Hypertension affects the retina, causing pathological remodeling (increased microvascular injury, fibrosis, and protein synthesis) and frequently leading to hypertensive retinopathy.<sup>1</sup> Although the management of hypertension can prevent the progression of retinopathy, there is currently no effective treatment for hypertensive retinopathy. In addition to hypertension, other factors play an important role in the development of hypertensive retinopathy. Extensive evidence indicates that inflammation, oxidative stress, and multiple signaling pathways [phosphoinositide 3-kinase/protein kinase B (AKT)/I $\kappa$ B kinase (IKK) $\beta$ /nuclear factor-kappa B (NF- $\kappa$ B)] are critical to the pathogenesis of hypertensive retinopathy.<sup>2-4</sup> Therefore, a strategy targeting these factors may provide significant clinical benefits for the treatment of this condition.

The ubiquitin–proteasome system (UPS) is a key protein degradation pathway in eukaryotic cells. It is involved in the regulation of cell proliferation, signal transduction, inflammation, and various physiological processes.<sup>5</sup> Ubiquitin C-terminal hydrolase L1 (UCHL1; also known as PGP9.5) is a deubiquitinating enzyme that specifically removes polyubiquitinated ubiquitin from target proteins to reduce their degradation, thereby regulating protein homeostasis. UCHL1 has been reported to be associated with hypertension and cardiovascular disease. For example, it

is present in atherosclerotic lesions from human carotid arteries and is considerably increased in the neointima of the balloon-injured carotid artery. Additionally, it participates in vascular remodeling via its regulation of inflammatory responses.<sup>6</sup> UCHL1 is also markedly upregulated in agonist-stimulated cardiomyocytes and hypertrophic and failing hearts, with UCHL1 knockdown significantly ameliorating cardiac hypertrophy and dysfunction. Cardiac hypertrophy and remodeling induced by transverse aortic constriction can be reversed by the UCHL1 inhibitor LDN57444 in wild-type mice.<sup>7</sup> Furthermore, LDN57444 strongly attenuates angiotensin II-induced hypertension, left atrial dilatation, fibrosis, inflammatory cell infiltration, and reactive oxygen species (ROS) production.<sup>8</sup> LDN57444 also improves cardiac hypertrophy and dysfunction in spontaneously hypertensive rats (SHRs).<sup>9</sup> These experiments suggest that UCHL1 mediates target organ damage in hypertension. However, its role in hypertensive retinopathy remains unclear.

In this study, we used SHRs as an animal model for hypertensive retinopathy. According to our previous observations, 6-month-old SHRs show hypertensive retinal changes, such as edema and arterial caliber alterations.<sup>10</sup> The UCHL1 inhibitor LDN57444 was applied to SHRs to investigate the effects and underlying molecular mechanism of UCHL1 in hypertensive retinopathy.

## Materials and methods

### *Animal experiments*

Twenty-eight Wistar–Kyoto (WKY) rats and 28 SHR (male, weighing 200–220 g) were purchased from Vitalriver Co., Ltd. (Beijing, China). All rats were maintained in an environment with a constant temperature ( $23 \pm 2^\circ\text{C}$ ) under a 12-hour light/dark cycle with free access to food and water. We measured the mRNA and protein levels of UCHL1 in the retina of WKY rats and SHRs at 1 month of age ( $n = 6$  per group). The same experiment was performed at 2 months of age ( $n = 6$  per group). For the 6-month experiments, the remaining WKY rats and SHRs at 2 months of age underwent blood pressure evaluation (baseline) and were then randomly divided into four groups: WKY+vehicle, WKY+LDN57444, SHR+vehicle, and SHR+LDN57444 ( $n = 8$  per group). The selective UCHL1 inhibitor LDN57444 (Selleck, Houston, TX, USA) was dissolved in corn oil for administration ( $20 \mu\text{g}/\text{kg}/\text{day}$ , intraperitoneal) to 2-month-old rats; this treatment was administered daily for an additional 4 months. Control rats received daily injections of corn oil without the inhibitor as a vehicle control. When the animals were 6 months old, they were anesthetized by pentobarbital overdose ( $100 \text{ mg}/\text{kg}$ , intraperitoneal), and the eyes were removed and prepared for further experiments.

All experiments were approved by the Animal Care and Use Committee of Dalian Medical University (AEE1-2016-045) and conformed to the National Institutes of Health Guide for the Care and Use of Laboratory Animals and the ARRIVE guidelines.

### *Blood pressure measurements*

Blood pressure and heart rate measurements were taken each week from 1

month of age until the end of the experiment at 6 months of age using the noninvasive tail-cuff method (BP-2010A; Softron, Tokyo, Japan) on a preheated plate at  $37^\circ\text{C}$  to dilate the tail artery as previously described.<sup>11</sup> The average of at least 5 successive measurements for each rat was taken as the individual blood pressure and heart rate values.

### *Histological analysis*

The eyes used for pathological examination were fixed in 4% paraformaldehyde overnight, embedded in paraffin, and sectioned at  $5 \mu\text{m}$ . The sections were stained with hematoxylin and eosin (H&E) and immunohistochemically stained with an anti-UCHL1 antibody (Santa Cruz Biotechnology, Dallas, TX, USA). To determine the ROS level in the retina, frozen sections ( $5 \mu\text{m}$  thick) were stained with dihydroethidium (DHE; Sigma-Aldrich, St. Louis, MO, USA) for 30 minutes at  $37^\circ\text{C}$  as previously described.<sup>2</sup> To detect endothelial cell proliferation in the retina, the frozen sections were also permeabilized with Dylight 594 Labeled Griffonia Simplicifolia Lectin I (GSL I) isolectin B4 (Vector Laboratories Inc., Burlingame, CA, USA) at  $4^\circ\text{C}$  for 12 hours and incubated with 4',6-diamidino-2-phenylindole (DAPI; Sigma-Aldrich) for 5 minutes at room temperature. We randomly selected four sections at least  $60 \mu\text{m}$  apart from each eye. Images were acquired with a BX53 microscope (Olympus, Tokyo, Japan), and the fluorescence intensities were quantified with ImageJ (National Institutes of Health, Bethesda, MD, USA).

### *RNA isolation and quantitative real-time PCR (qPCR) analysis*

Retinal tissues were detached from the eyes under a stereoscope at  $4^\circ\text{C}$ . Total RNA was extracted from retinas with TRIzol reagent

(Takara Bio, Kusatsu, Japan). cDNA was obtained using a GoScript™ reverse transcription kit (Promega, Southampton, UK) in accordance with the manufacturer's instructions. qPCR was performed on a 7500 Fast Real-Time PCR System (Applied Biosystems, Carlsbad, CA, USA) using a SYBR Green Master Mix (Takara Bio) as previously described.<sup>2</sup> Glyceraldehyde-3-phosphate dehydrogenase (GAPDH) was used as an internal control. Interleukin (IL)-1 $\beta$ , IL-6, tumor necrosis factor (TNF)- $\alpha$ , nicotinamide adenine dinucleotide phosphate (NADPH) oxidase 1 (NOX1), NOX2, and NOX4 primers were obtained from Sangon Biotech (Shanghai, China). The primer sequences are shown in Table 1.

### Western blotting analysis

Total protein was extracted from retinal tissues using radioimmunoprecipitation assay buffer containing phenylmethanesulfonyl fluoride as a phosphatase inhibitor (Beyotime Biotechnology, Shanghai, China). Protein concentrations were determined using the Abbkine Protein Quantification Kit (Thermo Fisher Scientific, Carlsbad, CA, USA). Equal amounts of extracted proteins (40  $\mu$ g) were separated by sodium dodecyl sulfate–polyacrylamide gel electrophoresis and

transferred to polyvinylidene fluoride membranes (Millipore, Billerica, MA, USA). The membranes were blocked with 5% bovine serum albumin (Sigma-Aldrich) for 60 minutes at room temperature and then incubated overnight at 4°C with anti-phospho-AKT (9271S), anti-AKT (9272S), anti-phospho-NF- $\kappa$ B-p65 (3033S), anti-NF- $\kappa$ B-p65 (4764S), anti-phospho-IKK $\alpha$ / $\beta$  (2697S), anti-IKK $\alpha$  (2682S), anti-IKK $\alpha$  (2678S), anti-hypoxia-inducible factor 1-alpha (HIF-1 $\alpha$ , 14179) (all from Cell Signaling Technology, Danvers, MA, USA), vascular endothelial growth factor (VEGF, JH121) (Invitrogen, Carlsbad, CA, USA), anti-NOX1 (ab131088), or anti-NOX2 (ab129068) antibodies (Abcam, Cambridge, MA, USA). All protein levels were normalized to those of GAPDH. Images were captured and quantified using ImageJ (National Institutes of Health).

### NOX activity

Samples were centrifuged at 8000  $\times$ g for 20 minutes, and the protein concentration was determined by the Bradford assay. The resulting particulate fraction was used to measure NOX activity. NOX activity in the retina was determined by luciferin (5  $\mu$ M) enhanced chemiluminescence, and the results were normalized for protein content.

**Table 1.** Primers for quantitative real-time PCR analysis

Gene	Forward Primer (5'-3')	Reverse Primer (5'-3')
<i>UCLH1</i>	CGGCCAGCATGAAAACCTC	TTATTGGCCACTGCGTGGAT
<i>IL-1<math>\beta</math></i>	CTCTGTGACTCGTGGGATGATG	CCACTTGTGGCTTATGTTCTGTC
<i>IL-6</i>	TCTGCTCTGGTCTTCTGGAG	TTGCTCTGAATGACTCTGGC
<i>TNF-<math>\alpha</math></i>	TGATCGGTCCCAACAAGGA	TGCTTGGTGGTTTGCTACGA
<i>NOX1</i>	GCTCCTAAGAGGCTCCAGAC	TGGGTGCATGACAACCTTGG
<i>NOX2</i>	CTGCCAGTGTGTCGGAATCT	AATGGCCGTGTGAAGTGCTA
<i>NOX4</i>	TGGCCAACGAAGGGGTAA	CACTGAGAAGTTCAGGGCGT
<i>GAPDH</i>	AGTGCCAGCCTCGTCTCATA	GATGGTGATGGGTTTCCCCT

UCLH1, ubiquitin C-terminal hydrolase L1; IL, interleukin; TNF, tumor necrosis factor; NOX, NADPH oxidase; GAPDH, glycerol-3-phosphate dehydrogenase.

## Statistical analysis

All data are expressed as means  $\pm$  standard error of mean (SEM). Parameters were compared using the unpaired Student's *t*-test or ANOVA. Data that did not meet the above conditions were analyzed using a nonparametric Mann–Whitney *U* test. *P* values less than 0.05 were considered statistically significant. All statistical analyses were performed using IBM SPSS Statistics for Windows, Version 22 (IBM Corp., Armonk, NY, USA).

## Results

### *UCHL1 expression is increased in the retina of SHR*

To investigate the critical role of UCHL1 in the regulation of retinopathy in SHR, we first measured the level of UCHL1 in the retina of SHR at different months. The retinal mRNA and protein levels of UCHL1 were similar at 1 month of age. However, they were significantly higher in SHR compared with WKY rats at 2 and 6 months of age ( $P < 0.05$ ) (Figure 1a–d). Similarly, immunostaining indicated that the UCHL1-positive area of the retina was larger in SHR compared with WKY rats at 6 months of age ( $P < 0.05$ ) (Figure 1e). These results suggest that increased UCHL1 levels in the retina may play an important role in hypertensive retinopathy in SHR.

### *Inhibition of UCHL1 expression attenuates hypertension and retinal morphology in SHR*

Previous studies have shown that SHR exhibit mild hypertension at 2 months of age but no significant damage to target organs, including the heart, kidneys, vessels, and retina. Subsequently, their blood pressure continues to increase, with clear damage to target organs at 6 months of

age.<sup>11,12</sup> To determine whether the inhibition of UCHL1 expression influences blood pressure and retinal morphology in SHR, we administered the UCHL1 inhibitor LDN54777 (20  $\mu$ g/kg/day) to SHR and WKY rats at 2 months of age and continued treatment for 4 months (Figure 2a). LDN57444-treated SHR showed significantly reduced systolic blood pressure, although the inhibitor did not normalize the hypertension to the level observed in WKY rats ( $P < 0.05$ ) (Figure 2b). Moreover, the retinas of SHR may develop hemorrhage, edema, hard exudates, and cotton-wool spots due to hypoxia and capillary permeability intensification.<sup>10</sup> H&E staining showed that the ganglion cell layer was loose and swollen. The thickness of the central retina (at two optic-disc diameters from the optic disc), particularly the inner plexiform, inner nuclear, and photoreceptor layers, was markedly increased in SHR. These elevations were significantly reduced in LDN57444-treated SHR ( $P < 0.05$ ) (Figure 2c). However, the peripheral retinal morphology and thickness in the 4 groups were similar (Figure 2d). Next, we used immunohistochemical staining to assess the inflammatory response in retinas. The accumulation of ionized calcium-binding adaptor molecule 1-positive microglia/macrophages was observed in vehicle-treated SHR; this accumulation was significantly attenuated in LDN57444-treated SHR ( $P < 0.05$ ) (Figure 2e). There were no significant differences in systolic blood pressure or retinal morphological changes in WKY rats between inhibitor- and vehicle-treated groups. These results suggest that LDN57444 treatment attenuates hypertension and hypertensive retinopathy in SHR.

### *UCHL1 inhibition reduces retinal oxidative stress, vascular permeability, and inflammation in SHR*

Oxidative stress, vascular permeability, and inflammation play critical roles in

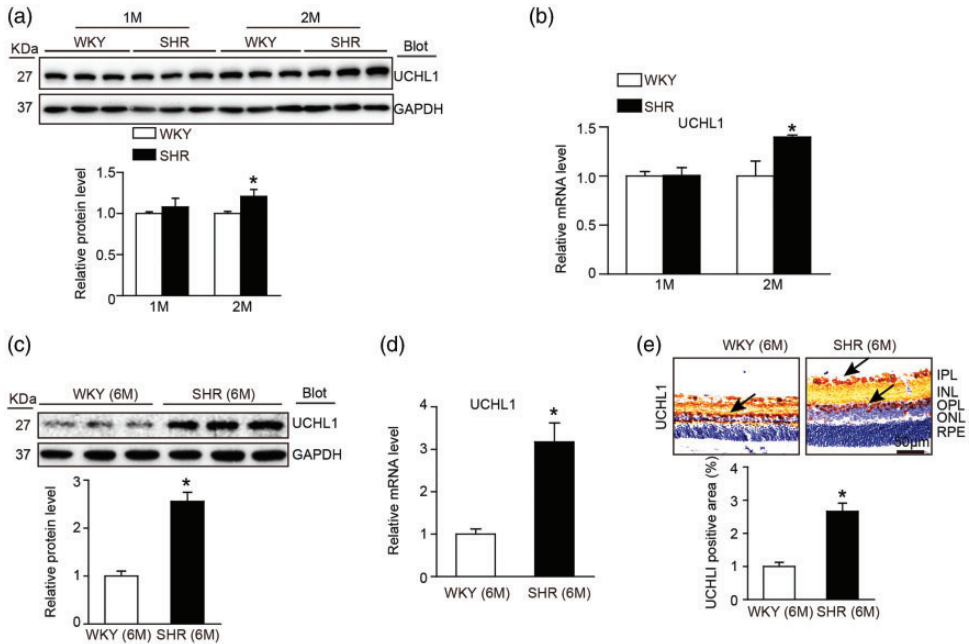


**Figure 1.** UCHL1 expression in the retina of WKY rats and SHRs. (a) Immunoblotting analysis of UCHL1 protein in the retina of WKY rats and SHRs at 1 and 2 months of age (**upper**). Quantification of the relative protein level (**lower**;  $n = 3$ ). (b) qPCR analysis of the mRNA level of UCHL1 in the retina of 1- and 2-month-old WKY rats and SHRs ( $n = 6$ ). (c) Immunoblotting analysis of UCHL1 protein in the retina of 6-month-old WKY rats and SHRs (**upper**). Quantification of the relative protein level (**lower**;  $n = 3$ ). (d) qPCR analysis of the mRNA level of UCHL1 in the retina of 6-month-old WKY rats and SHRs ( $n = 6$ ). (e) Immunohistochemical staining of the retina with an anti-UCHL1 antibody (**upper**). Quantification of the UCHL1-positive area (**lower**,  $n = 6$ ). Data are presented as means  $\pm$  SEM, and  $n$  represents the number of samples per group. \* $P < 0.05$  versus WKY rats

UCHL1, ubiquitin C-terminal hydrolase L1; WKY, Wistar-Kyoto; SHRs, spontaneously hypertensive rats; qPCR, quantitative real-time PCR; M, months; IPL, inner plexiform layer; INL, inner nuclear layer; OPL, outer plexiform later; ONL, outer nuclear layer; RPE, retinal pigment epithelium; GAPDH, glycerol-3-phosphate dehydrogenase.

promoting the occurrence and development of hypertensive retinopathy. Therefore, we examined the effect of UCHL1 inhibition on superoxide production and NOX activation in the retina of SHRs. LDN54777 treatment markedly reduced superoxide production and NOX activity compared with vehicle-treated SHRs, and these differences were mainly observed above the inner nuclear layer ( $P < 0.05$ ) (Figure 3a and 3b). Moreover, isolectin B4/DAPI staining revealed that endothelial cell proliferation

in inner retinas was significantly reduced in LDN57444-treated SHRs ( $P < 0.05$ ) (Figure 3c). We then evaluated the contribution of UCHL1 to retinal inflammatory responses. qPCR analysis indicated that the mRNA expression levels of proinflammatory cytokines (IL-1 $\beta$ , IL-6, and TNF- $\alpha$ ) were also significantly reduced in LDN54777-treated SHRs compared with vehicle-treated SHRs ( $P < 0.05$ ) (Figure 3d). We next analyzed the mRNA expression level of NOX isoforms by qPCR



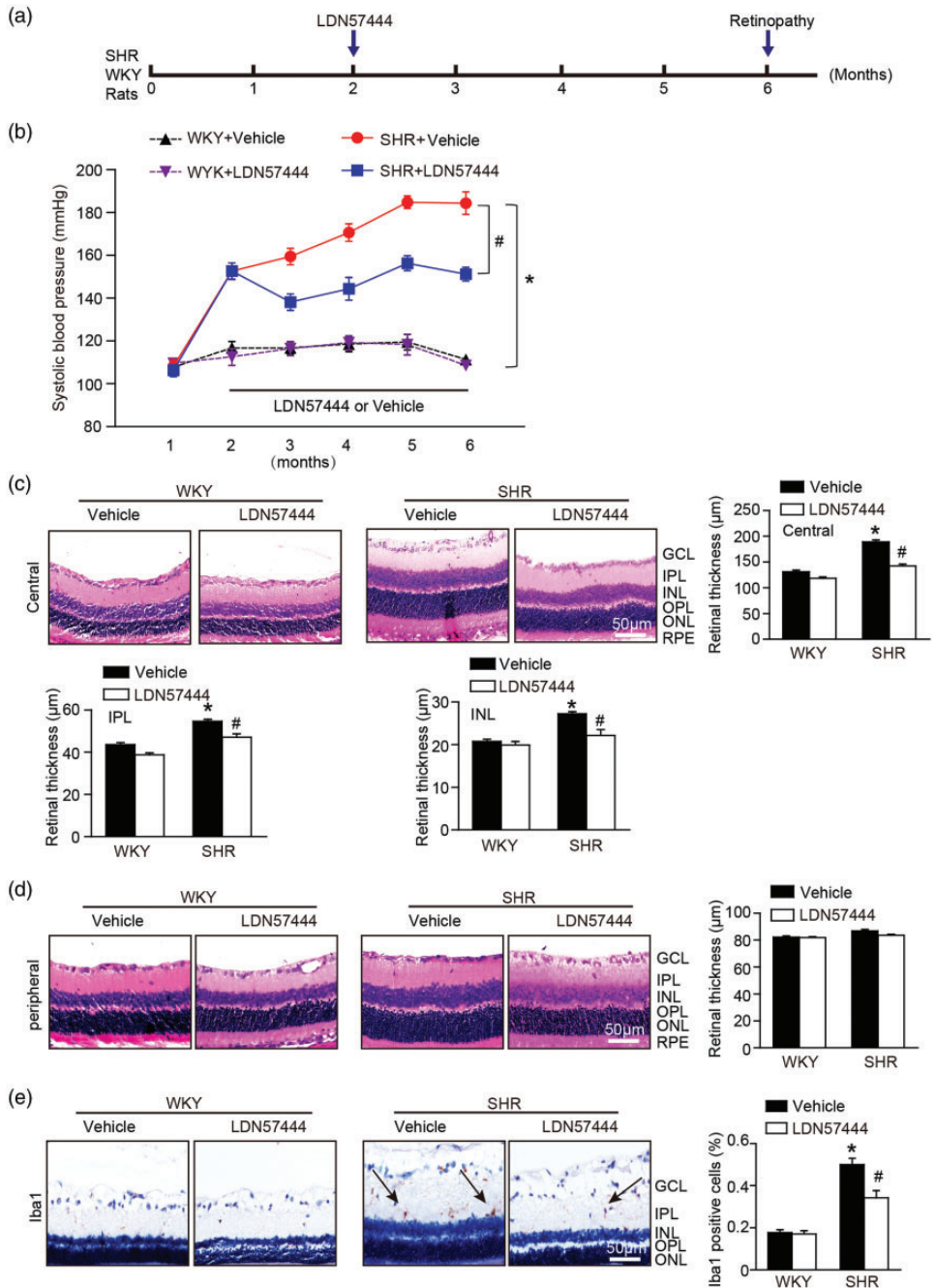


**Figure 2.** Pharmacological inhibition of UCHLI by LDN57444 attenuates hypertension, UCHLI expression, and retinal thickness. (a) WKY rats and SHRs at 2 months of age were intraperitoneally injected with the UCHLI inhibitor LDN57444 (20 µg/kg/day) or vehicle (corn oil) for 4 months. (b) Systolic blood pressure was measured every month using the tail-cuff method (n = 8). (c) Representative H&E staining of

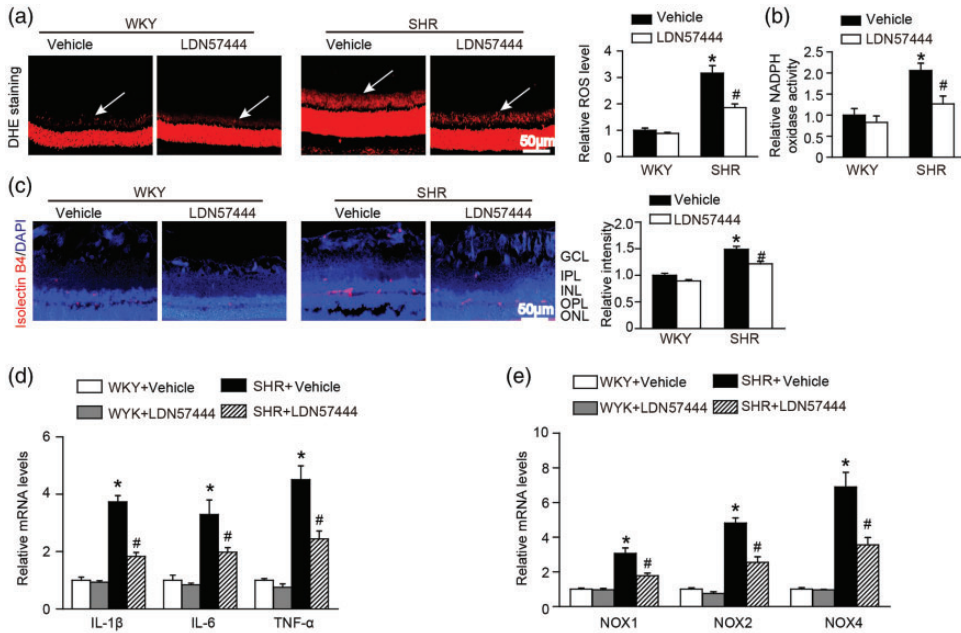


**Figure 3.** LDN57444 administration prevents retinal superoxide production and inflammation. (a) DHE staining of superoxide production (left). Quantification of the ROS level (right,  $n = 6$ ). (b) Measurement of NOX activity ( $n = 6$ ). (c) Representative isolectin B4 (red) staining of central retinal sections (left) and quantification of fluorescence intensity (right,  $n = 6$ ). Nuclei were counterstained with DAPI (blue). (d) qPCR analysis of the mRNA levels of IL-1 $\beta$ , IL-6, and TNF- $\alpha$  in the retina of WKY rats and SHRs ( $n = 4$ ). (e) qPCR analysis of the mRNA levels of NOX1, NOX2, and NOX4 in the retina of WKY rats and SHRs ( $n = 4$ ). Data are presented as means  $\pm$  SEM, and  $n$  represents the number of samples per group. \* $P < 0.05$  versus WKY rats, # $P < 0.05$  versus SHRs

DHE, dihydroethidium; ROS, reactive oxygen species; DAPI, 4',6-diamidino-2-phenylindole; SHRs, spontaneously hypertensive rats; WKY, Wistar-Kyoto; qPCR, quantitative real-time PCR; IL, interleukin; TNF, tumor necrosis factor; NOX, NADPH oxidase; GCL, ganglion cell layer; IPL, inner plexiform layer; INL, inner nuclear layer; OPL, outer plexiform later; ONL, outer nuclear layer; RPE, retinal pigment epithelium.

## Figure 2. Continued

central retinal sections (left) and quantification of central retinal thickness (right,  $n = 6$ ). (d) Representative H&E staining of peripheral retinal sections (left) and quantification of the retinal thickness (right,  $n = 6$ ). (e) Representative immunohistochemical staining of Iba1 (arrow) in the retinas (left) and quantification of Iba1-positive cells (right,  $n = 6$ ). Data are presented as means  $\pm$  SEM, and  $n$  represents the number of samples per group. \* $P < 0.05$  versus WKY rats, # $P < 0.05$  versus SHRs

UCHL1, ubiquitin C-terminal hydrolase L1; WKY, Wistar-Kyoto; SHRs, spontaneously hypertensive rats; H&E, hematoxylin and eosin; Iba1, ionized calcium-binding adapter molecule 1; GCL, ganglion cell layer; IPL, inner plexiform layer; INL, inner nuclear layer; OPL, outer plexiform later; ONL, outer nuclear layer; RPE, retinal pigment epithelium.



analysis and found that the retinal expression levels of NOX1, NOX2, and NOX4 were also significantly lower in LDN54777-treated SHR than in vehicle-treated SHR ( $P < 0.05$ ) (Figure 3e).

### **Administration of LDN57444 attenuates the activation of AKT/IKK/NF- $\kappa$ B signaling pathways**

Previous research has demonstrated that the protein levels of inflammatory signaling mediators (p-AKT, p- $\text{IKK}\alpha/\beta$ , and p-NF- $\kappa$ B) are critically linked to the development of hypertensive retinopathy through their regulation of proinflammatory cytokine and superoxide production.<sup>2</sup> To investigate the possible mechanism by which UCHL1 inhibition improves hypertensive retinopathy in SHR, we examined these signaling pathways. Immunoblotting showed that treatment of SHR with LDN54777 significantly reduced the protein levels of UCHL1, p-AKT, p- $\text{IKK}\alpha/\beta$ , and p-p65 in the retina compared with the vehicle ( $P < 0.05$ ) (Figure 4a). We next tested the effects of UCHL1 on retinal oxidative stress and vascular permeability. The protein levels of NOX1, NOX2, HIF-1 $\alpha$ , and VEGF were also significantly lower in LDN54777-treated SHR than in vehicle-treated SHR ( $P < 0.05$ ) (Figure 4b and 4c). Taken together, these results suggest that UCHL1 inhibition attenuates activation of the pathways associated with hypertensive retinopathy.

## **Discussion**

This study demonstrated the role of UCHL1 and its inhibitor LDN54777 in regulating hypertension and retinopathy in SHR. Our results showed that the mRNA and protein levels of UCHL1 in the retina were significantly increased in SHR compared with WKY rats from 2 months of age. Additionally, systolic

blood pressure, central retinal thickness, vascular permeability, inflammation, and superoxide production were significantly increased in the retina of SHR compared with WKY rats. In contrast, LDN54777 treatment markedly attenuated these effects. These beneficial actions were possibly associated with a reduction in blood pressure and the inactivation of multiple signaling pathways, including AKT,  $\text{IKK}\alpha/\beta$ , NF- $\kappa$ B, HIF-1 $\alpha$ , and VEGF. Collectively, increased expression of UCHL1 is an important determinant in the pathogenesis of hypertensive retinopathy, and its inhibition prevents disease progression, suggesting that UCHL1 is a potential therapeutic target for the treatment of hypertensive retinopathy.

Previous reports have suggested that the UPS plays a critical role in hypertension-related diseases.<sup>5,13</sup> As one of the major deubiquitinating enzymes, UCHL1 has multiple biological functions and is associated with neurodegenerative diseases, cancer, cardiovascular diseases, and retinopathy.<sup>14–16</sup> Previous studies have found that UCHL1 expression is enhanced in the pressure overload- and angiotensin II-treated heart and atrium in C57BL/6J mice<sup>7,17</sup> but decreased in the retina of diabetic rats.<sup>18</sup> However, the mechanism by which UCHL1 affects hypertensive retinopathy remains unclear. LDN54777 is a reversible and competitive inhibitor of UCHL1 hydrolase activity. Selective blockade of UCHL1 activity by LDN57444 has been demonstrated to delay Alzheimer's disease progression, impair cancer invasion, and improve cardiac hypertrophy and dysfunction.<sup>7,19,20</sup> In this study, daily LDN54777 administration to SHR from 2 to 6 months of age attenuated hypertension, central retinal thickness, vascular permeability, inflammation, and superoxide production by inhibiting the AKT,  $\text{IKK}\alpha/\beta$ , NF- $\kappa$ B, HIF-1 $\alpha$ , and VEGF signaling pathways (Figures 2–4). Thus, these results

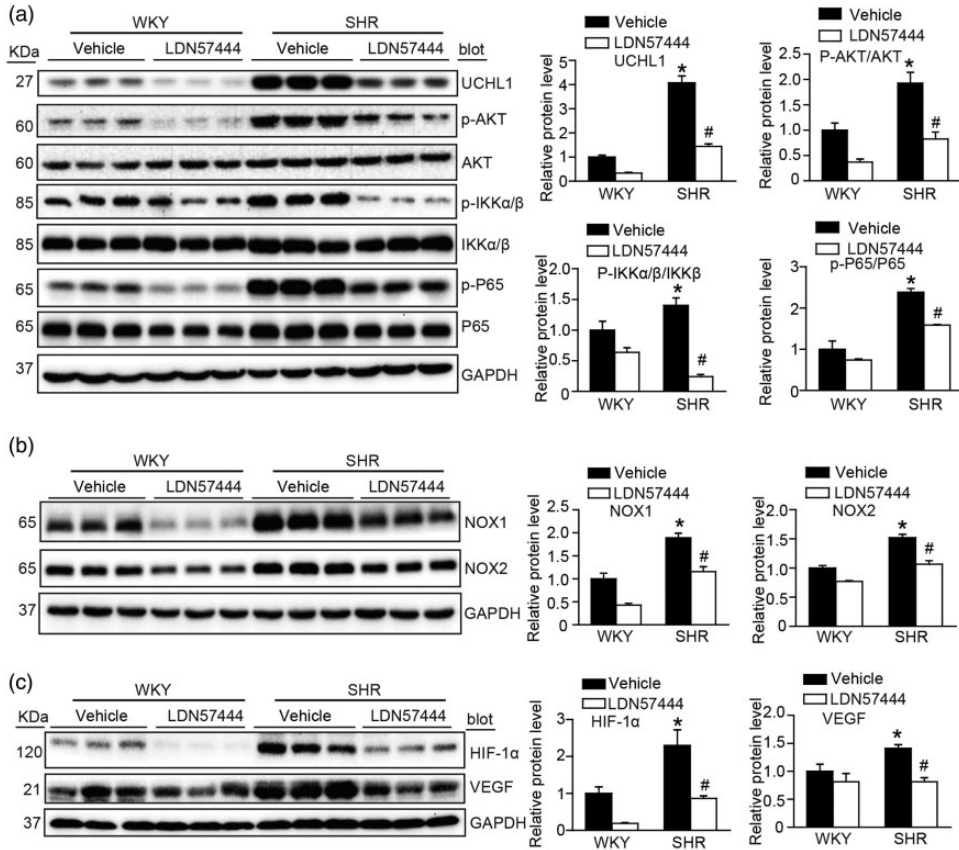


**Figure 4.** LDN57444 treatment inhibits the activation of proinflammatory signaling pathways in the retina of SHRs. (a) Immunoblotting analysis of UCHL1, p-AKT, p-IKK $\alpha/\beta$ , and p-p65 protein levels in the retina of 6-month-old WKY rats and SHRs (left). Quantification of each protein band (right,  $n = 4$ ). (b) Immunoblotting analysis of NOX1 and NOX2 expression in the retina of 6-month-old WKY rats and SHRs (left) and quantification of protein bands (right,  $n = 4$ ). (c) Immunoblotting analysis of HIF-1 $\alpha$  and VEGF expression in the retina of 6-month-old WKY rats and SHRs (left) and quantification of protein bands (right,  $n = 4$ ). GAPDH was used as an internal control. Data are presented as means  $\pm$  SEM, and  $n$  represents the number of samples per group. \* $P < 0.05$  versus WKY rats, # $P < 0.05$  versus SHRs. UCHL1, ubiquitin C-terminal hydrolase LI; SHRs, spontaneously hypertensive rats; WKY, Wistar-Kyoto; AKT, protein kinase B; IKK, I $\kappa$ B kinase; p, phosphorylated; NOX, NADPH oxidase; HIF-1 $\alpha$ , hypoxia-inducible factor 1 alpha; VEGF, vascular endothelin growth factor; GAPDH, glycerol-3-phosphate dehydrogenase.

indicate that UCHL1 provides a potential therapeutic target for the treatment of hypertension and hypertensive retinopathy.

Although elevated blood pressure is the main cause of hypertensive retinopathy, it cannot fully explain its pathogenesis. Other important mechanisms of hypertensive

retinopathy include oxidative stress, chronic inflammation, endothelial dysfunction, and vascular remodeling induced by hypertension/angiotensin II.<sup>21–23</sup> For example, IL-1 $\beta$  triggers involution of the choroid, which leads to severe hypoxia in the outer retina.<sup>24</sup> IL-1 $\beta$  also plays a regulatory role in immune

activation and inflammatory responses, together with IL-6 and TNF- $\alpha$ . IL-6 is involved in angiotensin II-induced activation of NOX and VEGF overexpression in the retina.<sup>25</sup> TNF- $\alpha$  induces the production of VEGF, which indirectly stimulates retinal angiogenesis<sup>26</sup> and increases retinal endothelial cell permeability.<sup>27</sup> ROS are ubiquitous signaling molecules in biological systems that play a role in promoting inflammation, endothelial cell proliferation and migration, and the formation of new blood vessels.<sup>28</sup> NOX enzymes (NOX1, NOX2, and NOX4), as the main source of ROS in retinal vascular endothelial cells, cause endothelial dysfunction, which leads to retinal morphological changes and dysfunction.<sup>29,30</sup> Our work revealed increased levels of proinflammatory cytokines (IL-1 $\beta$ , IL-6, and TNF- $\alpha$ ) and NOX isoforms (NOX1, NOX2, and NOX4) and enhanced endothelial cell proliferation in the retina of SHR at 6 months of age, which is consistent with previous findings.<sup>2,3</sup> Furthermore, we found that the levels of these factors were significantly lower in LDN54777-treated SHR compared with vehicle-treated SHR (Figures 3 and 4).

Multiple signaling pathways are activated in hypertensive retinopathy, including AKT, phosphatase and tensin homolog, NOX, transforming growth factor- $\beta$ /Smad, and NF- $\kappa$ B.<sup>31</sup> UCHL1 regulates the degradation of several proteins related to inflammation, oxidative stress, and arteriolar remodeling, including p53, I $\kappa$ B- $\alpha$ , and HIF1 $\alpha$ .<sup>32–34</sup> Through further exploration of the mechanism underlying UCHL1 action, we found that AKT phosphorylation and HIF-1 $\alpha$  levels were increased in the retina of SHR. This change was reversed in LDN54777-treated SHR, and the hypertensive retinal pathological alterations were less prominent than in the vehicle-treated SHR group. To determine how LDN54777 inhibits hypertensive retinopathy in SHR, we further analyzed multiple signaling pathways. Our study

demonstrated that LDN54777 significantly blocked the activation of AKT, HIF-1 $\alpha$ , and related signaling mediators (IKK $\alpha$ / $\beta$ , NF- $\kappa$ B, and VEGF). As an important upstream signaling component of inflammatory responses in hypertension, NF- $\kappa$ B activation triggers the expression and secretion of various inflammatory cytokines involved in every stage of the early immune response. NF- $\kappa$ B signaling appears to be a primary regulator of VEGF, IL-6, and NOX, thereby modulating oxidative stress and blood vessel function, resulting in the infiltration of inflammatory factors into target organs and activation of inflammation.<sup>35,36</sup> Therefore, our study provides novel insights into the regulation of retinopathy by UCHL1 in SHR.

In conclusion, our study shows for the first time that UCHL1 expression is significantly increased in the retina of SHR and provides new evidence for the critical role of UCHL1 in hypertension and retinopathy. UCHL1 inhibition not only significantly reduced hypertension but also ameliorated the increase in central retinal thickness, vascular permeability, inflammation, and oxidative stress. The possible mechanism is partially associated with the inhibition of AKT, IKK $\alpha$ / $\beta$ , NF- $\kappa$ B, NOX, HIF-1 $\alpha$ , and VEGF signaling pathways. Therefore, UCHL1 may be a promising therapeutic target for hypertensive retinopathy. Further studies are needed to elucidate the effect of UCHL1 on retinal vessel caliber and the role of UCHL1 in other animal models and human hypertensive retinopathy.

#### Declaration of conflicting interest


The authors declare that there is no conflict of interest.

#### Funding

The author(s) disclosed receipt of the following financial support for the research, authorship, and/or publication of this article: This research was supported by a grant from the China

Liaoning Nature Foundation (17-500-8-04 to Dr. He).

## ORCID iD

Shasha Liu  <https://orcid.org/0000-0003-1891-5543>

## References

1. Wong TY and Mitchell P. The eye in hypertension. *Lancet* 2007; 369: 425–435. DOI: 10.1016/S0140-6736(07)60198-6.
2. Wang S, Li J, Bai J, et al. The immunoproteasome subunit LMP10 mediates angiotensin II-induced retinopathy in mice. *Redox Biol* 2018; 16: 129–138. DOI: 10.1016/j.redox.2018.02.022.
3. Wang S, Li J, Wang T, et al. Ablation of Immunoproteasome beta5i Subunit Suppresses Hypertensive Retinopathy by Blocking ATRAP Degradation in Mice. *Mol Ther* 2020; 28: 279–292. DOI: 10.1016/j.ymthe.2019.09.025.
4. Yue J and Zhao X. GPR174 suppression attenuates retinopathy in angiotensin II (Ang II)-treated mice by reducing inflammation via PI3K/AKT signaling. *Biomed Pharmacother* 2020; 122: 109701. DOI: 10.1016/j.biopha.2019.109701.
5. Pohl C and Dikic I. Cellular quality control by the ubiquitin-proteasome system and autophagy. *Science* 2019; 366: 818–822. DOI: 10.1126/science.aax3769.
6. Takami Y, Nakagami H, Morishita R, et al. Ubiquitin carboxyl-terminal hydrolase L1, a novel deubiquitinating enzyme in the vasculature, attenuates NF-kappaB activation. *Arterioscler Thromb Vasc Biol* 2007; 27: 2184–2190. DOI: 10.1161/ATVBAHA.107.142505.
7. Bi HL, Zhang XL, Zhang YL, et al. The deubiquitinase UCHL1 regulates cardiac hypertrophy by stabilizing epidermal growth factor receptor. *Sci Adv* 2020; 6: eaax4826. DOI: 10.1126/sciadv.aax4826.
8. Bi HL, Zhang YL, Yang J, et al. Inhibition of UCHL1 by LDN-57444 attenuates Ang II-Induced atrial fibrillation in mice. *Hypertens Res* 2020; 43: 168–177. DOI: 10.1038/s41440-019-0354-z.
9. Han X, Zhang YL, Fu TT, et al. Blockage of UCHL1 activity attenuates cardiac remodeling in spontaneously hypertensive rats. *Hypertens Res* 2020; 43: 1089–1098. DOI: 10.1038/s41440-020-0486-1.
10. Tian T, Wu L and Xu L. Effects of triamcinolone acetate on P2X7R/NLRP3 pathway and fundus angiopathy in spontaneously hypertensive rats. *Rec Adv Ophthalmol* 2020; 40: 1125–1129. DOI: 10.13389/j.cnki.rao.2020.0250.
11. Zhang YL, Geng C, Yang J, et al. Chronic inhibition of chemokine receptor CXCR2 attenuates cardiac remodeling and dysfunction in spontaneously hypertensive rats. *Biochim Biophys Acta Mol Basis Dis* 2019; 1865: 165551. DOI: 10.1016/j.bbadis.2019.165551.
12. Herrmann HJ, Fiedler U and Blodner R. Pathogenesis of myocardial fibrosis in spontaneously hypertensive rats (SHR). *Eur Heart J* 1995; 16: 243–252. DOI: 10.1093/oxfordjournals.eurheartj.a060891.
13. Ying X, Zhao Y, Yao T, et al. Novel Protective Role for Ubiquitin-Specific Protease 18 in Pathological Cardiac Remodeling. *Hypertension* 2016; 68: 1160–1170. DOI: 10.1161/HYPERTENSIONAHA.116.07562.
14. Bedekovics T, Hussain S and Galardy PJ. Walking the tightrope: UCH-L1 as an mTOR inhibitor and B-cell oncogene. *Oncotarget* 2019; 10: 5124–5125. DOI: 10.18632/oncotarget.27154.
15. Graham SH and Liu H. Life and death in the trash heap: The ubiquitin proteasome pathway and UCHL1 in brain aging, neurodegenerative disease and cerebral Ischemia. *Ageing Res Rev* 2017; 34: 30–38. DOI: 10.1016/j.arr.2016.09.011.
16. Esteve-Rudd J, Campello L, Herrero MT, et al. Expression in the mammalian retina of parkin and UCH-L1, two components of the ubiquitin-proteasome system. *Brain Res* 2010; 1352: 70–82. DOI: 10.1016/j.brainres.2010.07.019.

17. Zhang X, Guo L, Niu T, et al. Ubiquitin carboxyl terminal hydrolyase L1-suppressed autophagic degradation of p21WAF1/Cip1 as a novel feedback mechanism in the control of cardiac fibroblast proliferation. *PLoS One* 2014; 9: e94658. DOI: 10.1371/journal.pone.0094658.
18. Shruthi K, Reddy SS and Reddy GB. Ubiquitin-proteasome system and ER stress in the retina of diabetic rats. *Arch Biochem Biophys* 2017; 627: 10–20. DOI: 10.1016/j.abb.2017.06.006.
19. Kobayashi E, Aga M, Kondo S, et al. C-Terminal Farnesylation of UCH-L1 Plays a Role in Transport of Epstein-Barr Virus Primary Oncoprotein LMP1 to Exosomes. *mSphere* 2018; 3: e00030-18. DOI: 10.1128/mSphere.00030-18.
20. Poon WW, Carlos AJ, Aguilar BL, et al. beta-Amyloid (A $\beta$ ) oligomers impair brain-derived neurotrophic factor retrograde trafficking by down-regulating ubiquitin C-terminal hydrolase, UCH-L1. *J Biol Chem* 2013; 288: 16937–16948. DOI: 10.1074/jbc.M113.463711.
21. Coban E, Nizam I, Topal C, et al. The association of low-grade systemic inflammation with hypertensive retinopathy. *Clin Exp Hypertens* 2010; 32: 528–531. DOI: 10.3109/10641963.2010.496519.
22. Karaca M, Coban E, Ozdem S, et al. The association between endothelial dysfunction and hypertensive retinopathy in essential hypertension. *Med Sci Monit* 2014; 20: 78–82. DOI: 10.12659/MSM.889659.
23. Matteucci A, Ricceri L, Fabbri A, et al. Eye Drop Instillation of the Rac1 Modulator CNF1 Attenuates Retinal Gliosis and Ameliorates Visual Performance in a Rat Model of Hypertensive Retinopathy. *Neuroscience* 2019; 411: 119–129. DOI: 10.1016/j.neuroscience.2019.05.021.
24. Zhou TE, Rivera JC, Bhosle VK, et al. Choroidal Involution Is Associated with a Progressive Degeneration of the Outer Retinal Function in a Model of Retinopathy of Prematurity: Early Role for IL-1 $\beta$ . *Am J Pathol* 2016; 186: 3100–3116. DOI: 10.1016/j.ajpath.2016.08.004.
25. Rojas M, Zhang W, Lee DL, et al. Role of IL-6 in angiotensin II-induced retinal vascular inflammation. *Invest Ophthalmol Vis Sci* 2010; 51: 1709–1718. DOI: 10.1167/iovs.09-3375.
26. Robinson R, Ho CE, Tan QS, et al. Fluvastatin downregulates VEGF-A expression in TNF- $\alpha$ -induced retinal vessel tortuosity. *Invest Ophthalmol Vis Sci* 2011; 52: 7423–7431. DOI: 10.1167/iovs.11-7912.
27. Ramos CJ, Lin C, Liu X, et al. The EPAC-Rap1 pathway prevents and reverses cytokine-induced retinal vascular permeability. *J Biol Chem* 2018; 293: 717–730. DOI: 10.1074/jbc.M117.815381.
28. Blaser H, Dostert C, Mak TW, et al. TNF and ROS Crosstalk in Inflammation. *Trends Cell Biol* 2016; 26: 249–261. DOI: 10.1016/j.tcb.2015.12.002.
29. Appukuttan B, Ma Y, Stempel A, et al. Effect of NADPH oxidase 1 and 4 blockade in activated human retinal endothelial cells. *Clin Exp Ophthalmol* 2018; 46: 652–660. DOI: 10.1111/ceo.13155.
30. Wei Y, Gong J, Xu Z, et al. Nrf2 promotes reparative angiogenesis through regulation of NADPH oxidase-2 in oxygen-induced retinopathy. *Free Radic Biol Med* 2016; 99: 234–243. DOI: 10.1016/j.freeradbiomed.2016.08.013.
31. Katsi V, Marketou M, Vlachopoulos C, et al. Impact of arterial hypertension on the eye. *Curr Hypertens Rep* 2012; 14: 581–590. DOI: 10.1007/s11906-012-0283-6.
32. Gao H, Hartnett S and Li Y. Ubiquitin C-Terminal Hydrolase L1 regulates myoblast proliferation and differentiation. *Biochem Biophys Res Commun* 2017; 492: 96–102. DOI: 10.1016/j.bbrc.2017.08.027.
33. Kim HJ, Kim YM, Lim S, et al. Ubiquitin C-terminal hydrolase-L1 is a key regulator of tumor cell invasion and metastasis. *Oncogene* 2009; 28: 117–127. DOI: 10.1038/onc.2008.364.
34. Nakashima R, Goto Y, Koyasu S, et al. UCHL1-HIF-1 axis-mediated antioxidant property of cancer cells as a therapeutic target for radiosensitization. *Sci Rep* 2017; 7: 6879. DOI: 10.1038/s41598-017-06605-1.



35. Queisser N and Schupp N. Aldosterone, oxidative stress, and NF-kappaB activation in hypertension-related cardiovascular and renal diseases. *Free Radic Biol Med* 2012; 53: 314–327. DOI: 10.1016/j.freeradbiomed.2012.05.011.
36. Yu XJ, Zhang DM, Jia LL, et al. Inhibition of NF-kappaB activity in the hypothalamic paraventricular nucleus attenuates hypertension and cardiac hypertrophy by modulating cytokines and attenuating oxidative stress. *Toxicol Appl Pharmacol* 2015; 284: 315–322. DOI: 10.1016/j.taap.2015.02.023.